

## Multigrid Wavelet-Based Natural Pixel Method for Image Reconstruction in Emission Computed Tomography

Chang Je Park, Jeong Hwan Park, and Nam Zin Cho

Korea Advanced Institute of Science and Technology  
Department of Nuclear Engineering  
373-1 Kusong-dong, Yusong-gu, Taejon, Korea 305-701  
Fax: +82-42-869-3810 E-mail: nzcho@sorak.kaist.ac.kr

### Abstract

*We describe a multigrid wavelet-based natural pixel (WNP) method for image reconstruction in emission computed tomography (ECT). The ECT is used to identify the tagged radioactive material's position in the body for detection of abnormal tissue such as tumor or cancer, as in SPECT and PET. With ECT methodology in parallel beam mode, we formulate a matrix-based reconstruction method for radionuclide sources in the human body. The resulting matrix for a practical problem is very large and nearly singular. To overcome this ill-conditioning, wavelet transform is considered in this study. Wavelets have inherent de-noising and multiscale resolution properties. Therefore, the multigrid wavelet-based natural pixel (WNP) method is very efficient to reconstruct image from projection data that is noisy and incomplete. We test this multigrid wavelet natural pixel (WNP) reconstruction method with the MCNP generated projection data for diagnosis of the simulated cancerous tumor.*

### I. Introduction

Internally administered radionuclides are used medically for imaging studies of various body organs and for non-imaging studies such as thyroid uptake and blood volume measurements. But we can make only indirect measurements by probing the object, e.g., with invisible radiation from radioactive sources. So an image reconstruction procedure is needed to process the projection data to form an image and so to facilitate the interpretation of the measurements.<sup>1</sup>

We may divide computed tomography into two categories: transmission computed tomography (TCT) and emission computed tomography (ECT). The fundamental physical difference between TCT and ECT is that both the source and the attenuating medium are unknown in ECT, whereas only the attenuating medium is unknown in TCT. The second important difference is that of available statistics. An ECT device collects approximately 10,000 times less data per transverse section image than TCT.<sup>1</sup> But the expected errors in much of the ECT work are 10% or greater. This is one of the reasons that the reconstruction strategy for ECT involves investigation of algorithms of the iterative class. Fig. 1 shows the configurations of ECT and TCT.

In this paper, we describe a multigrid and wavelet-based natural pixel (WNP) reconstruction technique for the ECT problem<sup>2</sup> with incomplete noisy projection data, that has been successfully used in the TCT problem.<sup>3</sup> The natural pixel (NP) representation results in a matrix-based reconstruction method which has the advantage that the resulting reconstructions are devoid of many of the incomplete data artifacts present in the tomographic reconstruction. But a disadvantage of the NP reconstruction is that it requires solutions of a very large, generally ill-conditioned system of equations. Since the projection

data (i.e., measurements) are usually noise-contaminated, this ill-conditioning is very troublesome for the numerical stability of the solutions. To overcome this ill-conditioning problem, wavelet transform and regularized wavelet multigrid are used in the reconstruction procedure.

Because of the space and frequency localization of wavelets which results from the multiresolution analysis, wavelets are very useful in many different fields of science and engineering.<sup>4</sup> This particular kind of dual localization achieved by wavelets renders the matrix representation of large classes of functions and operators sparse, or sparse to some high accuracy, when they are transformed into the wavelet domain. The sparse transformation matrix equation can then be easily solved by singular value decomposition (SVD). Singular value decomposition (SVD) is the method of choice for solving most of the linear least squares problems. In addition, the wavelet transform gives a desirable property of de-noising for noisy imaging problems, again due to the multiresolution analysis. The use of wavelet bases enables us to formulate a multiscale tomographic reconstruction method wherein the object is reconstructed at multiple scales or resolutions. The overall reconstruction is obtained by combining the reconstructions at different scales. This is the basic idea of wavelet multigrid method.

Among several wavelet bases, we have chosen the orthonormal compactly supported wavelets that were constructed by Daubechies.<sup>4</sup> For de-noising of the projection data a hard thresholding scheme is used. We apply our multigrid WNP reconstruction method to the projection data generated by MCNP.<sup>5</sup>

## II. Preliminaries of Wavelet Theory

Wavelets are very useful in many different fields of science and engineering, e.g., sound analysis and reconstruction, decomposition of visual data, PDE solver,<sup>6</sup> and detection of edges and singularities.<sup>7</sup> Here, we use wavelets for image reconstruction from incomplete and noisy projection data. Fundamentals of wavelet theory are provided in the following for completeness.

The wavelet functions are generated by dilation and translation operations such as

$$\psi_{n,k}(x) = 2^{-n/2} \psi(2^n x - k), \quad (1)$$

for some  $\psi \in L^2(\mathbf{R})$ .

A *multiresolution analysis (MRA)* of  $L^2(\mathbf{R})$  is defined as a set of closed subspaces  $V_j$  with  $j \in \mathbf{Z}$  that exhibit the following properties :

- 1)  $V_j \subset V_{j+1}$ ,
- 2)  $v(x) \in V_j \Leftrightarrow v(2x) \in V_{j+1}$  and  $v(x) \in V_0 \Leftrightarrow v(x+1) \in V_0$ ,
- 3)  $\bigcup_{j=-\infty}^{+\infty} V_j$  is dense in  $L^2(\mathbf{R})$  and  $\bigcap_{j=-\infty}^{+\infty} V_j = \{0\}$ ,
- 4) A scaling function  $\phi(x) \in V_0$  exists such that the set  $\{\phi(x-l) | l \in \mathbf{Z}\}$  is a basis of  $V_0$ .

Consequently, a sequence  $(h_k) \in l^2(\mathbf{Z})$  exists such that the scaling function satisfies a *two-scale difference equation*

$$\phi(x) = \sum_k h_k \phi(2x - k). \quad (2)$$

The set of functions  $\{\phi_{j,l}(x) | l \in \mathbf{Z}\}$  with  $\phi_{j,l}(x) = 2^{-j/2} \phi(2^j x - l)$  is an orthonormal basis of  $V_j$ . A complementary space of  $V_j$  in  $V_{j+1}$  is denoted by  $W_j$ , so that  $V_{j+1} = V_j \oplus W_j$ , and consequently,

$$\bigoplus_{j=-\infty}^{+\infty} W_j = L^2(\mathbf{R}). \quad (3)$$

The complementary spaces are chosen such that

$$w(x) \in W_j \Leftrightarrow w(2x) \in W_{j+1} \quad \text{and} \quad w(x) \in W_0 \Leftrightarrow w(x+1) \in W_0. \quad (4)$$

A function  $\phi(x)$  is a mother wavelet if the set of functions  $\{\phi(x-l) \mid l \in \mathbf{Z}\}$  is an orthonormal basis of  $W_0$ . Since the mother wavelet is also an element of  $V_l$ , a sequence  $(g_k) \in \ell^2(\mathbf{Z})$  exists such that

$$\phi(x) = \sum_k g_k \phi(2x-k). \quad (5)$$

The set of functions  $\{\psi_{j,l}(x) \mid l \in \mathbf{Z}\}$  with  $\psi_{j,l}(x) = 2^{j/2} \phi(2^j x - l)$  is an orthonormal basis of  $W_j$ . The coefficients  $h_k$  and  $g_k$  are related, for Daubechies' wavelet of order  $N$ , by

$$g_k = (-1)^k h_{2N-1-k}. \quad (6)$$

Now, suppose that a finite sequence  $s_k^0, k=1,2,\dots,K$ , is given. The fast wavelet transform (FWT)<sup>4</sup> can be written as:

$$\begin{aligned} s_k^j &= \sum_{n=0}^{2N-1} h_n s_{n+2k-1}^{j-1}, \\ d_k^j &= \sum_{n=0}^{2N-1} g_n s_{n+2k-1}^{j-1}, \end{aligned} \quad (7)$$

and the inverse fast wavelet transform can be written as:

$$\begin{aligned} s_{2n}^{j-1} &= \sum_{k=1}^N h_{2k-1} s_{n-k+1}^j + \sum_{k=1}^N g_{2k-1} d_{n-k+1}^j, \\ s_{2n-1}^{j-1} &= \sum_{k=1}^N h_{2k-2} s_{n-k+1}^j + \sum_{k=1}^N g_{2k-2} d_{n-k+1}^j, \end{aligned} \quad (8)$$

where  $N$  is the Daubechies' order. A wavelet transform of a 2-dimensional matrix is most easily obtained by performing 1-dimensional wavelet transform on the column vectors, then on the row vectors.<sup>8</sup>

### III. ECT Image Reconstruction

Emission computed tomography (ECT) can be used to determine the location of abnormal tissues or the moment-to-moment changes in chemistry and flow physiology by injected or inhaled compounds labeled with radioactive atoms. The field of ECT is generally considered a subject of nuclear medicine wherein until recently only projection images of the organ distribution of injected isotopes were used to estimate normal and abnormal tissues.

Suppose that we do not know where the radiation source is, nor how much attenuation exists between the source and the body edge. But we can only use the projection data of the original source, and from the projection data we want to reconstruct the original source distribution in the medium by indirect analysis. So ECT method is introduced, which needs to rotate the imaging device to get projection data at various angles.

For a parallel-beam imaging geometry, the projection data consists of parallel and non-overlapping strip integrals through the object that contains the radiation source at various angles.

The integral equation for projection data is as follows:

$$y_k(l) = \int \int_{\Omega} f(u, v) T_{kl}(u, v) A_{kl}(u, v) dudv, \quad k=1, \dots, N_\theta; \quad l=1, \dots, N_s, \quad (9)$$

where

$f(u, v)$  : object that contains radiation source to be reconstructed,

$y_k(l)$  : observation corresponding to projection  $l$  at angular position  $k$ ,

$T_{kl}(u, v)$  : indicator function of the strip integral corresponding to observation,

$A_{kl}(u, v)$  : attenuation function of the medium to the detector.

In our study, we consider operator  $T$  as track length in the pixel which the projection line goes through. Attenuation function  $A$  can be written as follows:

$$A_k(u, v) = \exp(-\mu(u, v)r(u, v; k, l)), \quad (10)$$

where

$\mu(u, v)$  : uniform attenuation factor in the position  $(u, v)$ ,

$r(u, v; k, l)$  : distance between the detector and the position  $(u, v)$ .

If we discretize Eq. (9), then the overall observation equation becomes

$$y = [y_1^T y_2^T \cdots y_{N_\theta}^T] = T_A f, \quad (11)$$

where

$f: N_s^2$  vector representing  $f(u, v)$  on an  $N_\theta \times N_s$  square pixel lattice,

$y: N_\theta N_s$  vector containing the projection data,

$T_A: N_\theta N_s \times N_s^2$  matrix representing the complete set of discretized attenuated indicator functions

$$\{T_{Akl}(u, v) \equiv T_{kl} A_{kl}; k=1, \dots, N_\theta; l=1, \dots, N_s\}.$$

The tomographic reconstruction problem is then to find an estimate  $\hat{f}$  of the discretized object  $f$  given the projection data contained in  $y$ . The natural pixel (NP) method is a class of matrix-based reconstruction method, which is expressed in implicit form as

$$y = (T_A T_A^T)x = Cx, \quad (12)$$

where  $\hat{f} = T_A^T x$ .

In this NP method, incomplete data is allowed and the matrix  $C$  is calculated for each specific acquisition geometry. But it is usually difficult to solve for  $x$ , because the size of matrix  $C$  is large with  $N_\theta N_s \times N_\theta N_s$  and it requires a tremendous amount of storage. It also usually results in an ill-conditioned problem.

#### IV. Multigrid Wavelet-Based Natural Pixel Reconstruction

It will be helpful if we transform the matrix  $C$  in Eq. (12) so that it may be inverted in a computationally efficient manner. So, we will use the wavelet transform. First, the noise-contaminated measurement data  $y$  is de-noised by wavelet transform.

The wavelet transform of the strip attenuated basis function is as follows:

$$\begin{aligned} \mathcal{J} &\equiv WT_A \\ &= [\mathcal{J}_1^T \mathcal{J}_2^T \cdots \mathcal{J}_{N_\theta}^T], \end{aligned} \quad (13)$$

where  $W$  is matrix representation of 1-D wavelet transform.

We define the vectors:

$$\eta \equiv Wy, \quad \xi \equiv Wx. \quad (14)$$

From Eqs. (12) and (14),

$$\eta = \Gamma \xi, \quad (15)$$

where the multiscale system matrix  $\Gamma$  is given by:

$$\Gamma = WCW^T = W(T_A T_A^T)W^T = \mathcal{J}\mathcal{J}^T. \quad (16)$$

Using the regularized least squares (RLS), the solution of Eq. (15) is given by

$$(\Gamma^T \Gamma + \lambda I)\hat{\xi} = \Gamma^T \eta, \quad (17)$$

where  $\lambda$  is a regularization parameter.

The size of the matrices in Eq. (17) is very large. So we would not solve it directly because of the memory problem in the computer. So we use wavelet multigrid method. Wavelet decomposition of a signal (or a vector) leads to a multiresolution representation of the signal (or the vector). If we exploit the multiresolution property, the computational time may be reduced. In this paper, we use V-cycle wavelet multigrid algorithm. The principle of this algorithm is illustrated in Fig. 2. Instead of the downward (from fine to coarse)

restriction in the classical V-cycle multigrid, where the error is calculated and restricted, here we use wavelet decomposition to reach the coarsest grid of the V-cycle. At the vertex of the V-cycle, SVD is used to find  $\xi$  (that is  $x$ ). In the case of the upward reconstruction (from coarse to fine), we use wavelet reconstruction instead of error prolongation (error compensation). In the wavelet multigrid method, the low frequency component is used assuming the other components are zero. In clinical applications, usually only certain regions with abnormal features are of interest. This wavelet multigrid algorithm allows to zoom-in to the special regions of interest (ROI's).

## V. Application and Conclusions

We apply the multigrid WNP reconstruction method to the ECT problem for simulated cancer detection in human body. Projection data are generated with the MCNP code.<sup>5</sup> From the projection data (uncollided flux in MCNP), we reconstruct cancerous tumors distribution, which are assumed of circular shape and located somewhere in the body. The results are shown in Fig. 3.

From the MCNP simulation, we find that the reconstruction of cancerous tumor with noiseless complete data (the size of matrix  $T_A$  is  $1024 \times 1024$ ) is sufficiently accurate. Even in the case of incomplete projection data (the size of matrix  $T_A$  is  $768 \times 1024$ ) with some noises, the multigrid WNP (wavelet-based natural pixel) reconstruction method gives accurate tumor image. We also find that the wavelet de-noising property is very effective in recovering the original image.

## References

1. G.T. Herman, *Image Reconstruction from Projections: Implementation and Applications*, Springer-Verlag, New York, 1979.
2. C.J. Park and N.Z. Cho, "Image Reconstruction in Emission Computed Tomography via Multigrid Wavelet-Based Natural Pixel Method," to be presented at *International Conference on the Physics of Nuclear Science and Technology*, Long Island, New York, October 1998.
3. N.Z. Cho and C.J. Park, "A Wavelet-Based Image Reconstruction in Transmission Computed Tomography," *Proceedings of the 1998 ANS Radiation Protection and Shielding Division Topical Conference: Technologies for the New Century*, Nashville, April 1998.
4. I. Daubechies, "Orthonormal Bases of Compactly Supported Wavelets," *Comm. Pure. Appl. Math.*, 41, 909-966, 1988.
5. J.F. Briesmeister, Ed., "MCNP - A General Monte Carlo N-Particle Transport Code, Version 4B," LA-12625-M, Los Alamos National Laboratory, 1997.
6. N.Z. Cho and C.J. Park, "Wavelet Theory for Solution of the Neutron Diffusion Equation," *Nuclear Science and Engineering*, 124, pp.417-430, 1996.
7. C.J. Park and N.Z. Cho, "Wavelet Transform Decomposition and Denoising for Reactor Monitoring," *Trans. Am. Nucl. Soc.*, 76, p.345, 1997.
8. C.J. Park and N.Z. Cho, "Fast Solution of Linear Systems by Wavelet Transform," *Proceedings of the Korean Nuclear Society Spring Meeting*, Vol. I, pp.282-287, May 1996, Cheju.

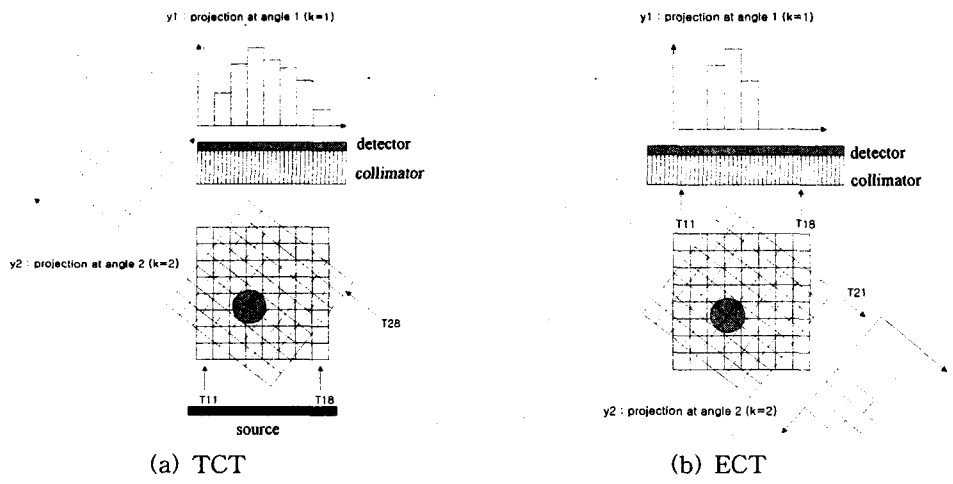


Fig. 1. Configuration of computed tomography

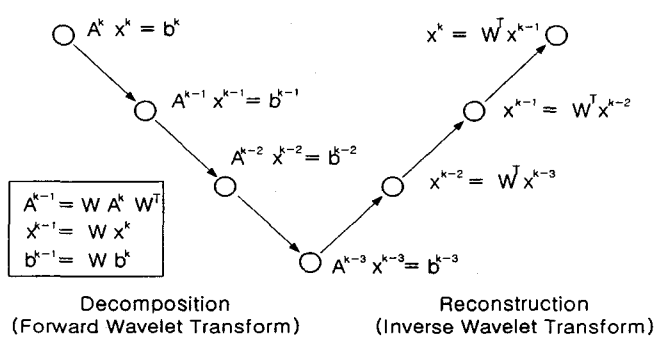
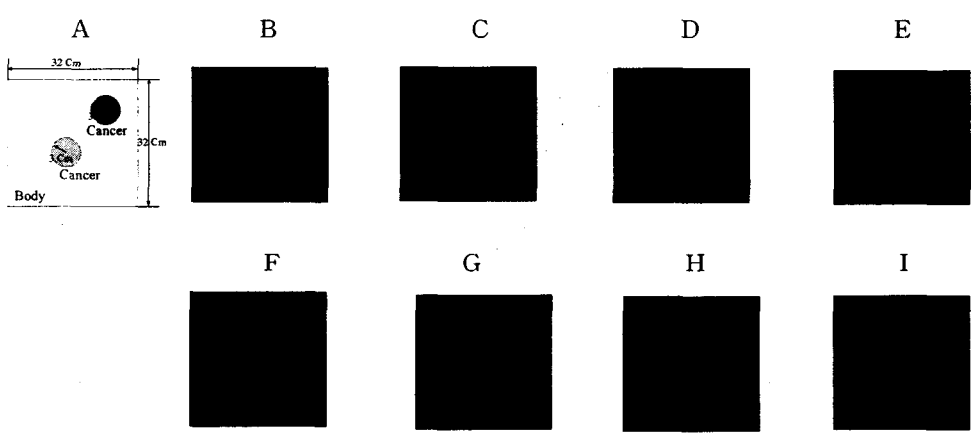


Fig. 2. Configuration of wavelet multigrid V-cycle



- A : Original image
- B : WNP (complete data, no noise, no multigrid)
- C : WNP (complete data, noise, no multigrid)
- D : WNP (complete data, no noise, multigrid :2 grids)
- E : WNP (complete data, noise, multigrid: 2 grids)
- F : WNP (incomplete data, no noise, no multigrid)
- G : WNP (incomplete data, noise, no multigrid)
- H : WNP (incomplete data, no noise, multigrid: 2 grids)
- I : WNP (incomplete data, noise, multigrid: 2 grids)

Fig. 3. Results of MCNP simulation (pixel size: 32×32)